Hot Superheavy Nuclei Seen with the GDR γ-Decay

MAJ, A; TVETER, TS; GAARDHOJE, JJ; HERSKIND, B; SLETTEN, G; RAMSOY, T; ATAC, A; KORTEN, W; BRACCO, A; CAMERA, F

Published in:
Acta Physica Polonica B

Publication date:
1995

HOT SUPERHEAVY NUCLEI SEEN WITH THE GDR γ-DECAY*

A. MAJ[a,b], T.S. TVETER[b,g], J.J. GAARDHØJE[b], B. HERSKIND[b], G. SLETTEN[b], T. RAMSØY[b], A. ATAÇ[b], W. KORTEN[b], A. BRACCO[c], F. CAMERA[c], M. MATTIUZZI[c], B. MILLION[c], M. PIGNANELLI[c], J. BACELAR[d], A. BUDA[d], H.v.D. PLOEG[d], W. KRÓLAS[a], H. NIFENECKER[e], F. SCHUSSLER[e], J.A. PINSTON[e], A. MENTHE[e], P. PAUL[f], D.J. HOFMAN[f], I. DIOSZEGI[f], S. SCHADMAND[f]

[a] H. Niewodniczański Institute of Nuclear Physics
Radzikowskiego 152, 31-342 Kraków, Poland

[b] Niels Bohr Institute, Blegdamsvej 17, DK-2100 Copenhagen Ø, Denmark

[c] Dipartimento di Fisica, Universitá di Milano e INFN Sezione Milano
Via Celoria 16, I-20133 Milano, Italy

[d] Kernfysisch Versneller Instituut
Zernikelaan 25, 9747AA Groningen, The Netherlands

[e] Institut des Science Nucleaires
Av. des Martyrs 53, F-38026 Grenoble, France

[f] Department of Physics, Nuclear Structure Laboratory
SUNY Stony Brook NY 11794, USA

[g] Department of Physics, University of Oslo, Blindern, N-1000 Oslo, Norway

(Received December 30, 1994)

The GDR gamma decay of highly excited ^{272}Hs and ^{269}Ns nuclei and their evaporation daughters was studied in coincidence with fission fragments. A difference technique was used to isolate the pre-fission component. Strong dipole collectivity was observed. The lifetime of the hot superheavy nuclei is estimated.

PACS numbers: 24.30.Cz, 25.70.Gh, 25.70.Jj

---

* Presented at the XXIX Zakopane School of Physics, Zakopane, Poland, September 5–14, 1994.

1. Introduction

The γ-decay of the Giant Dipole Resonance (GDR) built on excited states of a nucleus has been found to be a very useful tool to investigate certain collective properties of the nucleus (see for example [1–3]). Figure 1 shows the commonly used Yrast plot, excitation energy versus angular momentum, in which the regions of various nuclear behaviour are indicated. Close to the yrast line, where the nucleus is governed by the shell structure, the spectrum shape of the GDR γ-decay provides information on the shape of the nucleus, the shape evolution when the angular momentum is changing and on the scale of the shape fluctuations. The loss of shell effects, happening when the nucleus is warmed up, is reflected by the shape phase transition, from prolate or spherical to oblate, and is also manifested in the GDR spectrum. In this region an important quantity is the level density. It can be deduced either from the charged particle evaporation spectra [4], from first generation of gamma rays [5], or likewise from the GDR spectra [1, 2]. Very high in this plot, at a certain critical temperature, the thermal energy of nuclei is high enough that the nucleons can vaporize. One would have expected that this would have been associated with the disappearance of the GDR. It was found however [2] that the collective strength of the GDR vanishes well before this temperature is reached. This unexpected phenomenon has been associated with the loss of collectivity in the nucleus. At somewhat lower excitation energy (300 MeV) the increase of the GDR width saturates, what was found to be associated with the limit of angular momentum that nuclei can sustain without fission [6].

In this paper we will concentrate on another region of behaviour of nuclei shown in this plot, a region where nuclei are unstable with respect to fission. This subject is not new in GDR study. In fact, the history of hot Giant Resonances started in the spontaneously fissioning nuclei of ^{252}Cf [7] with $Z = 98$. New interest has come out in studying the GDR decay in fissioning nuclei as it allows to gain new insights into the process of fission. In fact, high energy γ-rays can be emitted both by the compound nucleus prior to fission and by the fission fragments.

A nucleus can fission either because it is rotating very fast or because it has a high charge. In our studies we concentrated on nuclei having very high charge, the *superheavy nuclei* with $Z \approx 108$. The technique of studying the pre-fission GDR decay, if the GDR will have time to build up in such heavy compound systems formed in heavy ion reactions, might give us a new information on superheavy elements, on the lifetime of hot superheavy conglomerate and on the process of fission.

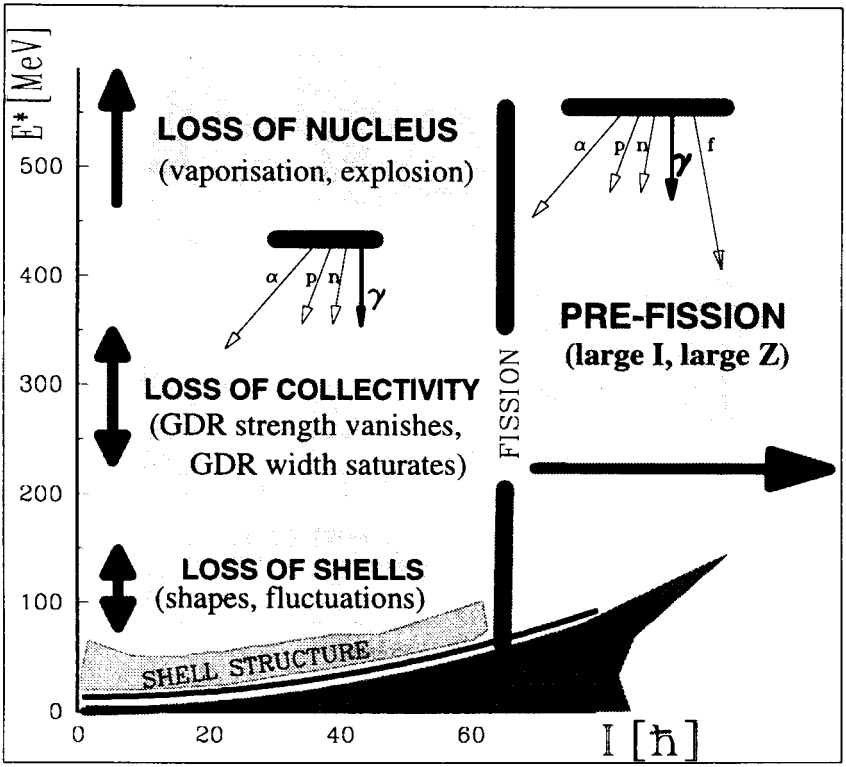

Fig. 1. A schematic plot of typical behaviour of nuclei in the excitation energy — angular momentum plane.

2. Fission timescales from neutron and GDR spectra

Why should we think that there will be time enough for GDR γ-emission before the compound system fissions? For a long time fission was believed to be a fast process, that can be treated in the statistical model similar to charged particle and neutron evaporation, just by ascribing to it a certain decay width. In the last few years however it has been realized that fission is a rather slow process. The most convincing indication came from the neutron spectra measured by the Berlin group [8]: through measurements of the angular distribution of the evaporated neutrons, pre-scission neutrons (having a symmetric angular distribution in the CM-frame) could be separated from the post-scission neutrons. Figure 2 shows them as a function of initial excitation energy of the compound nucleus, for systems with different Z. One can see, that an increase of the initial excitation energy of the compound nucleus results in a linear increase of the pre-scission neutron

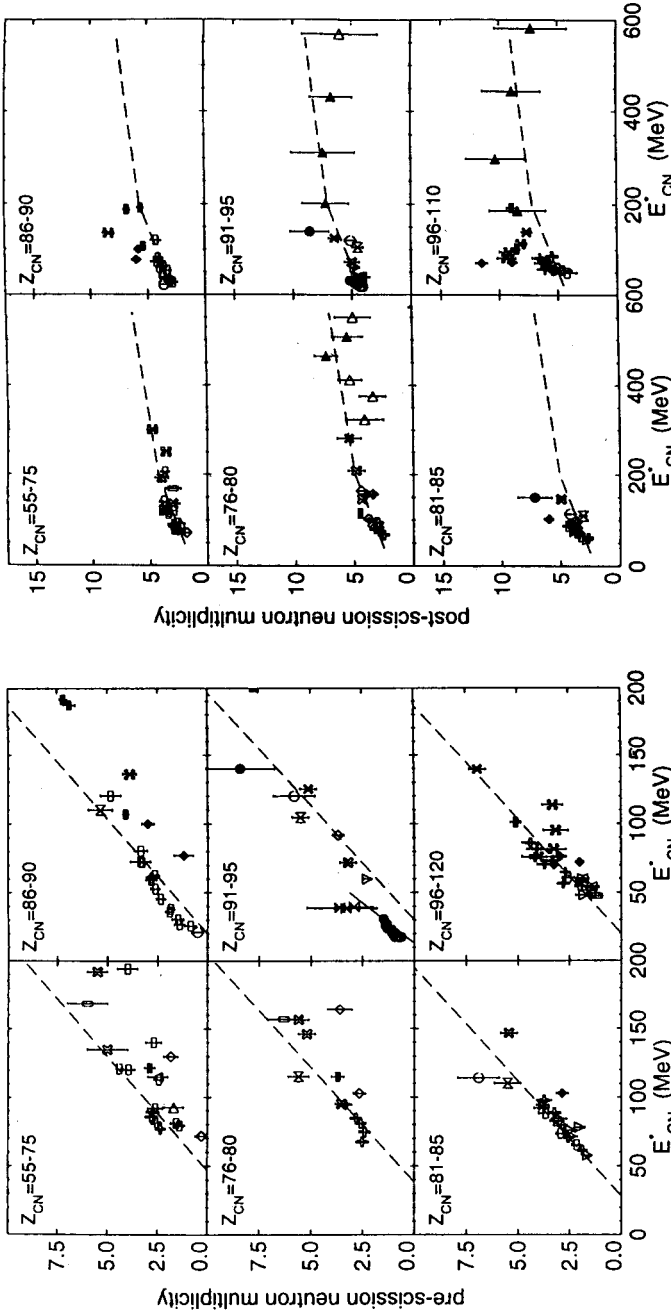

Fig. 2 Multiplicity of pre-scission (left hand side) and post-scission (right hand side) neutrons as a function of the initial excitation energy for systems with different Z (from [8]).

multiplicity, while the post-scission multiplicity saturates at a certain excitation energy. Also the number of pre-scission neutrons is much larger than predicted by the usual statistical model. This means that fission occurs very late in the decay of excited nucleus. The delay of the fission process has been understood as due to a slow large scale mass diffusion process governed by nuclear viscosity.

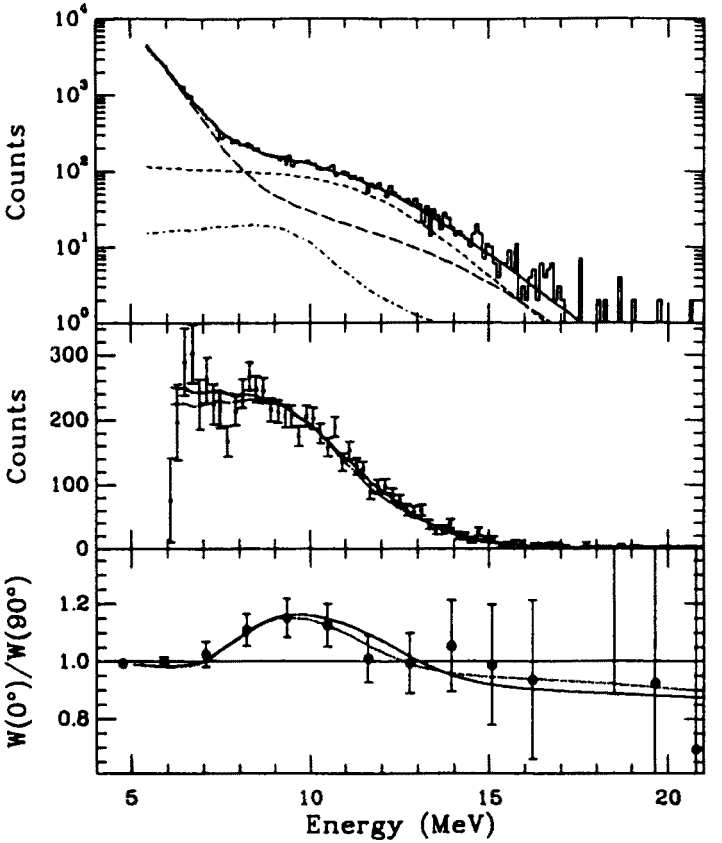

Fig. 3. Total gamma-ray spectrum (top), prefission contribution (middle) and the fission-γ-ray correlation pattern (bottom) from the 140 MeV ^{16}O on ^{208}Pb reaction (from [9]).

This idea was confirmed also by the measurements of the GDR γ-decay spectra done by the Stony Brook group [9]. Figure 3 shows an example of the observed spectrum in the reaction of 140 MeV ^{16}O on ^{208}Pb and the fission-gamma angular correlation. The reaction produces ^{224}Th at the initial excitation energy of 82 MeV. The lines are the results from the modified statistical code CASCADE, that includes the dissipation formalism and the

tracing of the deexcitation of fission fragments. The calculated contributions from the fission fragments are subtracted from the experimental spectrum, a clean GDR contribution from the fused compound nucleus is seen. A fission-γ-ray angular correlation spectrum exhibits a pattern typical for a dipole emission from a deformed system.

These findings seem to indicate that even in heavier nuclei, if we can create the system with an energy that is higher than the energy at which fission occurs, we might be able to see the gamma rays preceding the fission process.

3. The experiments

In order to produce superheavy elements in heavy ion reactions projectiles with masses $A > 40$ are required. Normally one uses energies close to the Coulomb barrier, in order to populate rather cold compound nuclei and at the same time reduce the probability of fission and evaporation of particles; and then identifies the meta-stable residua. The consequence, however, of such an approach is a very low production cross-section.

We decided to go to higher bombarding energies, above 7 MeV/nucleon. In this case the fusion cross section increases very rapidly [10]. We have, however, to pay a price that the nuclei are produced at high excitation energy and evaporate numerous particles. But since we could expect that the fission will occur very late, the compound system might hold for a significant amount of time so that it can be studied before it fissions, by for example measuring the γ-rays associated with the decay of the Giant Dipole Resonance built on the excited states of the compound system.

The experiments concerning this topic were performed within the HECTOR collaboration (Denmark, Italy and Poland), which has been established around the HECTOR detection system, built by the Niels Bohr Institute, Copenhagen and Milano University. We have performed three experiments, two with the SARA cyclotron at the ISN in Grenoble in which the hot compound system ^{272}Hs ($Z = 108$) was formed and one in Stony Brook in which ^{269}Ns ($Z = 107$) was produced. The reactions used were, respectively, ^{40}Ar+^{232}Th at 6.8, 10.5, 15.0 MeV/u, and ^{37}Cl+^{232}Th at 7.3 MeV/u.

The experimental set-up used in the Grenoble experiments is shown in Figure 4. As the beam hits the target, many different kinds of reaction take place. One of them, which we want to select, is the formation of the compound system that afterwards fissions. The fission fragments are detected in 4 position sensitive gas detectors: Parallel Plate Avalanche Counters (PPAC). The high energy gamma rays emitted from the compound system and from the fission fragments are measured in 8 large BaF_2 detectors

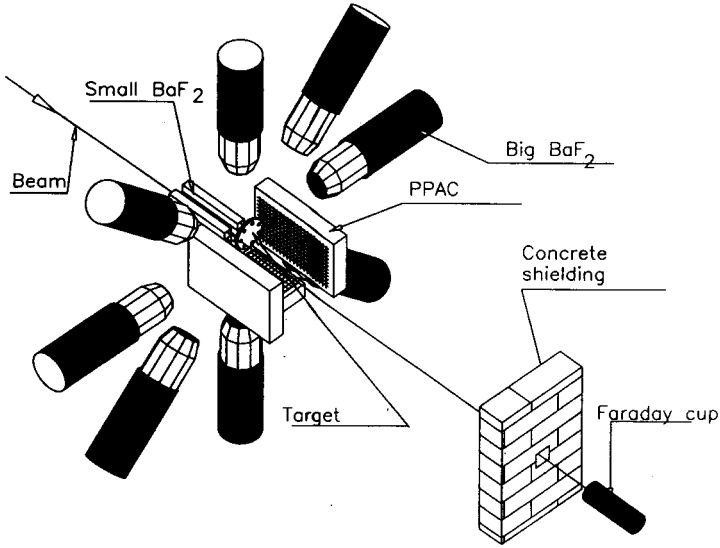

Fig. 4. Experimental set-up in the Grenoble experiment (see text for explanation). Upper PPAC detector was removed from the plot to see the location of the target wheel relative to the detectors.

(from the HECTOR array [11]) placed at 30 cm from the target. Another 7 small BaF_2 crystals (from KVI Groningen) were placed inside the reaction chamber close to the target. These detectors were used to measure the low energy gamma rays and to provide an efficient reaction time reference. The set-up used for the Stony Brook experiment was similar in concept.

In the experiment an event was accepted when both fission fragments were detected in the two opposite PPAC detectors. From the measured time of flight (from target to PPAC) and velocity directions of the fragments, one can calculate on the event-by-event basis the fragments' kinetic energies. Assuming binary reaction and knowing the CM velocity, one can evaluate the mass, the kinetic energy and the turning angle of each fragment, and the total kinetic energy in the output channel. Since the reactions which we are interested in, *i.e.* going through the compound system formation, are characterized by symmetric mass distribution of the fission products and by the 90° turning angle in CM, subsequently only the events fulfilling these conditions were sorted out.

The gamma spectra, measured in the large BaF_2 detectors in coincidence with the fission fragments contain the high energy gamma-rays emitted both from the heavy compound system *before* fission, and *after* fission, from the hot fission fragments. This makes a problem in disentangling of the pre-fission and post-fission components because GDR centroids in nuclei with $A = 272$ (the mass of superheavy system) and in nuclei with $A = 136$

(symmetric fission products) differ only by 3–4 MeV, while the typical GDR widths in hot nuclei are of the order of 6–12 MeV. One needs, for example, to fit the total experimental spectrum with the full statistical decay calculations that include also the decay of the fission fragments (see [9]).

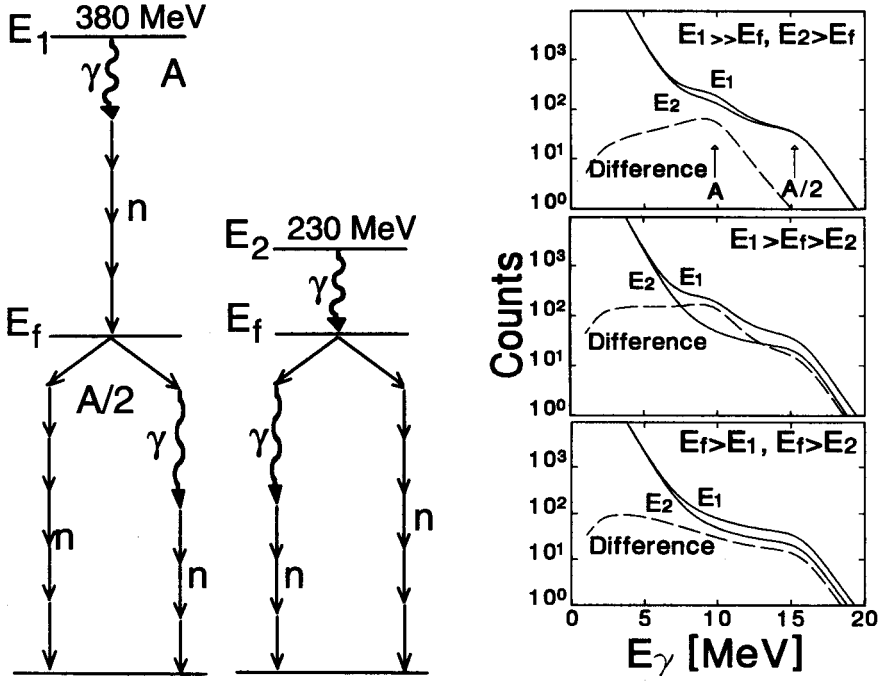

Fig. 5. The idea of the differential method explained in the text.

We have chosen a different approach: *the energy differential method*, which is explained in Figure 5. The main idea is based on the expectation that, since fission is a slow process, it only occurs when the system has cooled significantly by the faster particle evaporation. Two reactions employing the same projectile-target combination at two different bombarding energies are performed. In one the excitation energy E_1 of the compound nucleus will be high, for example 380 MeV. The excited nucleus will cool down evaporating neutrons and charged particles, and possibly gammas from GDR decay, until a certain excitation energy E_f where fission sets on. At this point 2 excited fission fragments are produced that can evaporate particles and gamma rays from GDR decay. In the second reaction the excitation energy E_2 is lower than E_1, say 230 MeV, but still higher than E_f. In this case the energy E_f, at which fission sets in, is reached after smaller number of decay steps. This scenario is illustrated in the left part of the figure. We measure the total γ-spectra in both reactions. After proper normalization

we can create a difference of the total gamma spectra (upper right part of the Figure 5). The post fission part will be identical in both spectra and will cancel out in the difference. The resulting difference spectrum should contain only the part not common to the two reactions, the part of γ-rays which are emitted *before fission* by the hotter system. This is the first, the most ideal scenario for studying the hot system prior to fission. We assume here that the typical excitation energy at which fission starts to play a role does not depend significantly on the initial excitation energy. This seems to be indeed the case as suggested by the post- and pre-fission neutrons analysis [8].

In the second possible scenario the "fission" energy E_f is higher than the excitation energy E_2 in the second nucleus. Thus in the low energy reaction the fission is a competing channel even at high excitation energies. Since the excitation energy of the fission fragments in the second reaction is lower than in the first, the number of possible post-fission decays is also lower, and the post-fission contribution will not cancel out completely in the difference (see middle right part of the Figure 5). If this scenario is experimentally observed, it gives the excitation energy region in which fission occurs.

In the third scenario, where E_f is higher than both E_2 and E_1 (or the concept of delayed fission is wrong), there will be no pre-fission part, and the difference spectra will contain gamma rays emitted from the few first decays of the excited fragments produced in the high energy reaction (lower right part of the Figure 5).

Performing a number of experiments with different bombarding energies, and using the differential method one can scan the excitation energy and find the excitation energy region, where fission sets in.

4. Results and discussion

4.1. Selecting fusion-fission events

Figure 6 shows the two-dimensional spectra of the products from the 7.3 MeV/u ^{37}Cl on ^{232}Th reaction (performed in Stony Brook). Figure 6(a) displays the calculated turning angle (in CM) of the fission fragment versus its mass, while in Figure 6(b) the total kinetic energy (TKE) in the output channel (sum of the kinetic energies of both fragments detected in opposite PPAC detectors) is plotted versus the mass of one of them. The gamma spectra obtained by setting narrow gates on these 2-dimensional fission fragments spectra (see Figure 6(c)) are displayed in the Figure 6(d). Gate #1 was set around mass $A = 136$ and around most probable Total Kinetic Energy. The other two gates were set on very asymmetric events. In the spectrum gated by symmetric fission the GDR bump is clearly visible,

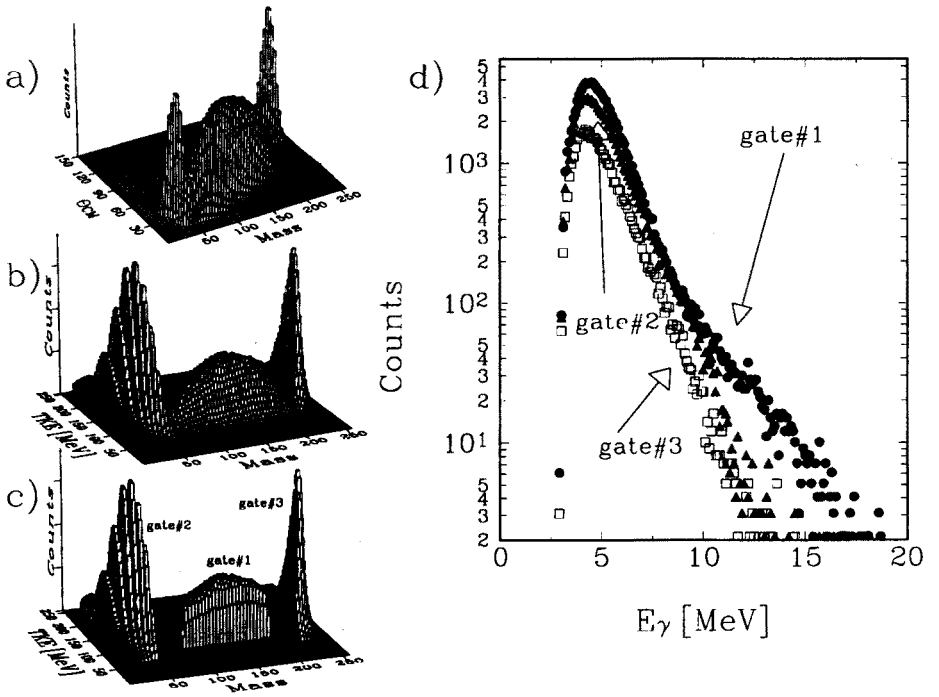

Fig. 6. Left hand side shows 2-dimensional spectra of the reaction products measured in PPAC detectors: (a) reaction product turning angle in CM *vs.* product masses; (b) reaction total kinetic energy *vs.* product masses; (c) same as (b) but with 3 gates set. On the right hand side (d) are shown high energy gamma ray spectra obtained in coincidence with 3 different gates on the 2-dimensional spectra: full circles correspond to the symmetric fission (gate#1 in (c)), full triangles -light mass fragments (gate#2), hollow squares - heavy mass fragments (gate#3).

while in the two other gates, the spectra show mostly exponential behaviour, typical for rather cold nuclei. It can be seen indeed that the selection of symmetric fission events enhances the highest excitation energies, and therefore the compound nucleus formation channel. For the final analysis, gates were set both on the *TKE-A* spectra and on the θ_{CM}-*A* spectra around $\theta_{CM} = 90°$.

4.2. Total and difference GDR spectra

The left side of the Figure 7 shows the spectrum, measured in the first experiment [12] at the bombarding energy of 6.8 MeV/u (corresponding to the initial excitation energy of the compound nucleus of approximately 110 MeV) in coincidence with the symmetric fission fragments. Note that

the yield of γ-rays in the interval 8–13 MeV is smaller at the 6.8 MeV/u reaction, as expected. The lines show statistical model predictions of the gamma rays coming from the fission fragments, assuming that they are excited to 60 (short-dashed line) and 80 MeV (long-dashed line). It seems that the 60 MeV line approximates the high energy part reasonably well. However, in order to reproduce the entire spectrum, a prefission component seems to be needed. On the right hand side we see the spectrum (also from the first run in Grenoble) for the 10.5 MeV/u reaction. Here the lines are: statistical model analysis for the fission fragments, excited to $E^* = 80$ MeV (long-dashed line); an estimate of the pre-fission component for mass $A = 272$ and excitation energy of 230 MeV (short-dashed line); the sum of these two components (solid line). We find here that in order to reproduce the experimental spectrum both components are needed. In this run the statistics was rather poor, so the difference spectrum could not be created.

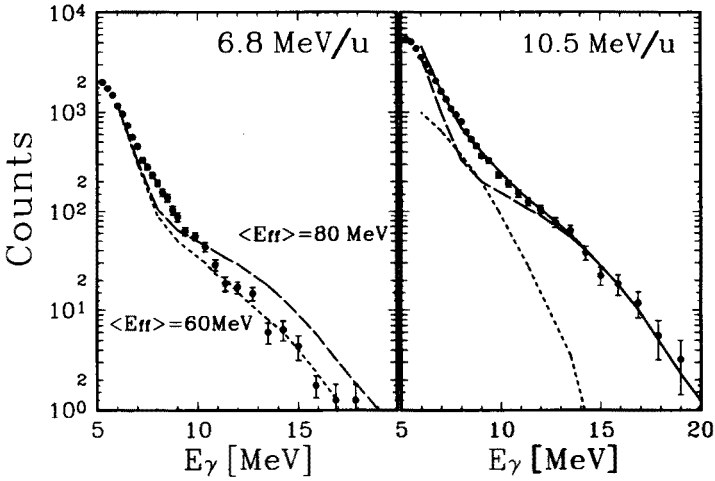

Fig. 7. Measured gamma ray spectra gated by symmetric fission (from [11]). Left hand side shows spectrum for the reaction at 6.8 MeV/u compared to simple statistical model calculations for the fission fragments, assuming the excitation energies of the fragments from symmetric fission of 60 (short dashed) and 80 MeV (long dashed), respectively. Right hand side shows similar spectrum for the reaction at 10.5 MeV. Long dashed curve represents the calculation for the fission fragments with 80 MeV excitation energy, short dashed curve shows estimate of the pre-fission component and the solid curve indicates the sum of the two contributions.

Figure 8 shows the comparison of the results from the second run performed in Grenoble [13] at 15.0 and 10.5 MeV/u together with the 6.8 MeV/u reaction from the previous experiment. All spectra are, as before,

in coincidence with the detection of symmetric fission in PPAC's. Spectra have been normalized based on the absolute gamma ray multiplicities per reaction which is determined in the experiment.

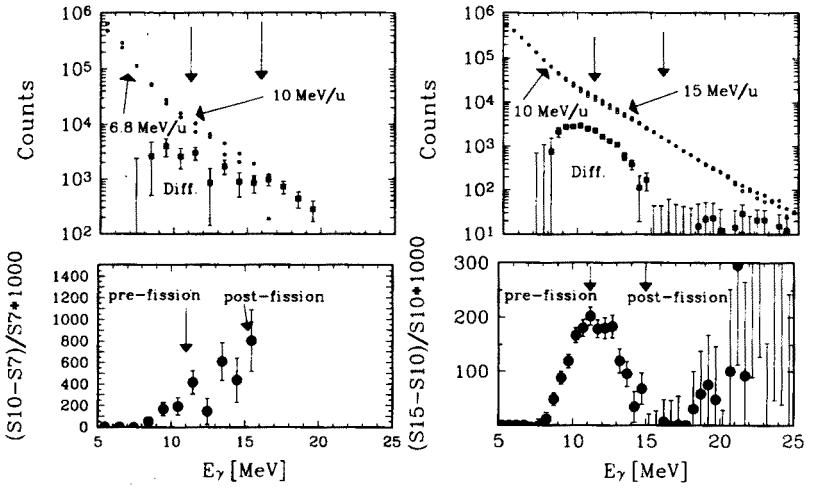

Fig. 8. Comparison of the gamma-ray spectra gated by symmetric fission obtained at three different bombarding energies: 15.0, 10.5 and 6.8 MeV/u. In the top left panel are compared the spectra from 10 MeV/u (full circles) and 6.8 MeV/u (hollow circles) reaction, and their difference (full squares) is shown. This difference, divided by the spectrum at 6.8 MeV/u for showing it in the linear scale, is presented in the bottom left panel. Similarly in the top right panel are the spectra from 15 MeV/u and 10.5 MeV/u together with their difference, and in the bottom right panel their relative (divided by spectrum at 10.5 MeV/u) difference is shown.

The left hand side of the figure shows the comparison of the spectra at the two lower bombarding energies (6.8 MeV/u, 10.5 MeV/u). The difference between the two spectra is shown in logarithmic scale in the upper panel. A linear representation is obtained by dividing the difference spectrum by the spectrum at lower bombarding energy and shown in the lower left panel of the figure. Although the counting statistics in the reaction at 6.8 MeV/u is insufficient above 15 MeV, it is nevertheless quite clear that some pre-fission emission is present. It also appears that fission still competes at these energies as may be recognized by the rise in the difference yield around 15 MeV (the expected energy of the GDR in the fission fragments). Thus in the excitation energy range 110–230 MeV, scenario number two (middle right panel of Figure 5) seems most appropriate to describe the observation.

The situation is much clearer in the comparison of the two higher energies (10.5 MeV/u and 15.0 MeV/u) shown in the right hand side. In this case it appears that the post-fission yield indeed cancels out in the subtraction, disclosing clearly the presence of the pre-fission GDR component. The observed centroid of the component is in excellent agreement with the expected GDR resonance energy for the heavy composite system ($E_{\mathrm{GDR}}(A = 272) \approx 12.2$ MeV). Here definitely scenario number one (upper right panel and left part of Figure 5) is realized.

4.3. Fission — gamma-ray angular correlation

As we learned from the talk of Angela Bracco [3], the angular distribution pattern of the GDR γ-rays can provide us with the information: *i)* whether we indeed have to do with dipole radiation, *ii)* on the type of deformation of the studied system (prolate or oblate), *iii)* on the orientation of rotation with respect to the symmetry axis of the nucleus (collective, non-collective). In the case of fissioning nuclei it is possible to measure the angular distribution of γ-rays with respect to the direction of the total angular momentum instead of doing it with respect to the beam axis, as it is usually done for fusion-evaporation reactions. The total angular momentum direction is determined by knowing the fission axis, since the most probable direction of fission products is perpendicular to the angular momentum vector. The fission axis is determined by the pair of opposite PPAC detectors that have fired. This is illustrated in Figure 9. One usually represents the fission — γ-ray angular correlation by plotting the anisotropy $W(0°)/W(90°)$ as a function of γ-ray energy, *i.e.* the ratio of spectra measured at 0° and 90°. With the set-up we have used the anisotropy is obtained by comparing spectra detected in the same BaF_2 detector. The spectrum for $\theta(\gamma - I_{\mathrm{rot}}) = 90°$ is obtained by gating on the pair of PPAC detectors that is aligned with the BaF_2 (left and right PPAC detector in Figure 9), while for $\theta(\gamma - I_{\mathrm{rot}}) = 0°$ one uses a gate on the other pair of PPACs, that is aligned perpendicularly to the previous pair (top and bottom). It is a big advantage to be able to compare in the same experimental run spectra from the same detector, because this eliminates the problem of different absolute efficiency and the energy dependence of the efficiency, as it is the case when using different detectors.

The lower part of the Figure 9 shows the expected anisotropy for different nuclear shapes and orientations, both for the systems with $A = 272$ and $A = 130$. The calculations were done assuming that the nuclei have shapes with deformation parameter $\beta = 0.4$ for $A = 272$ and $\beta = 0.2$ for $A = 130$. The width of the GDR component was assumed to be 5 MeV.

It is necessary, however, to correct the measured spectra for neutron pile-up before the angular distribution can be obtained. The pile-up arises

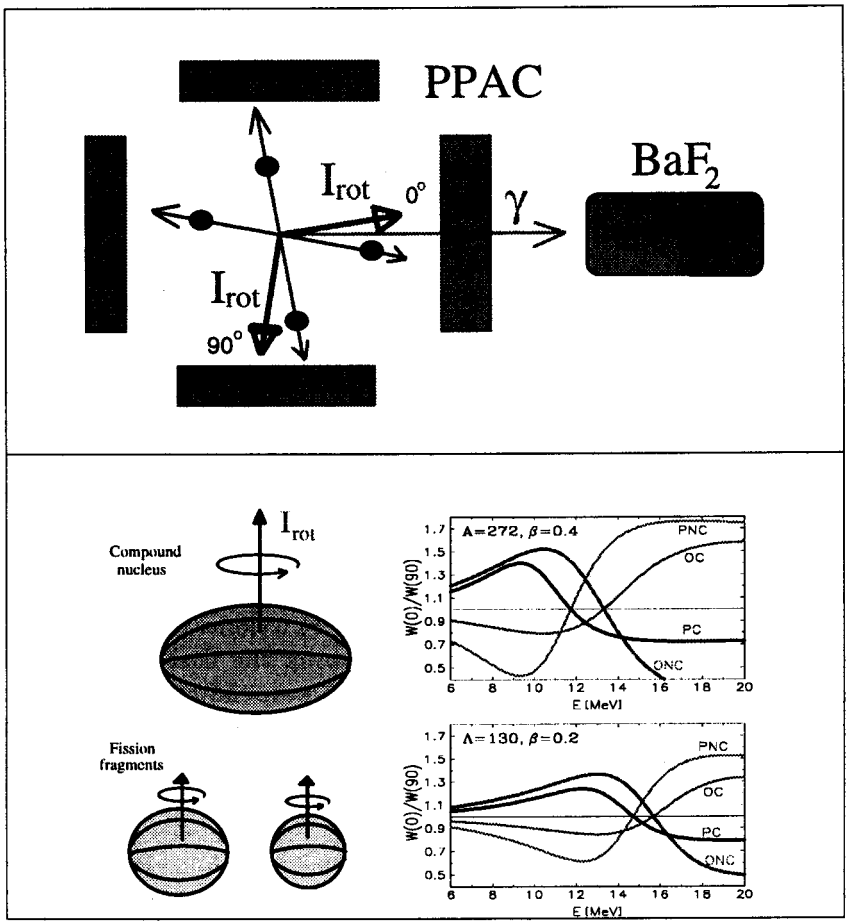

Fig. 9. Idea of the angular distribution measurement. In the upper part is shown the experimental arrangement, in which it is possible to measure the anisotropy W(0°)/W(90°) of the gamma radiation with respect to the direction of the spin I_{rot}, using only one BaF_2 detector (see text for details). In the bottom part are shown the calculated patterns of the angular anisotropy both for superheavy nuclei (A=272, with the assumed deformation parameter β=0.4) and for fission fragments (A=130, β=0.2). Prolate collective rotation is denoted by PC, oblate non-collective by ONC, prolate non-collective by PNC and oblate collective by OC.

from the special geometry of the set-up, in which some of the detectors are placed behind the PPAC detectors. This is schematically illustrated in Figure 10. The left hand side shows 3 "snapshots" of the fusion-fission reaction process. The reaction is observed (upper snapshot) by 2 PPAC detectors in which fission fragments are measured, and 2 BaF_2 detectors in

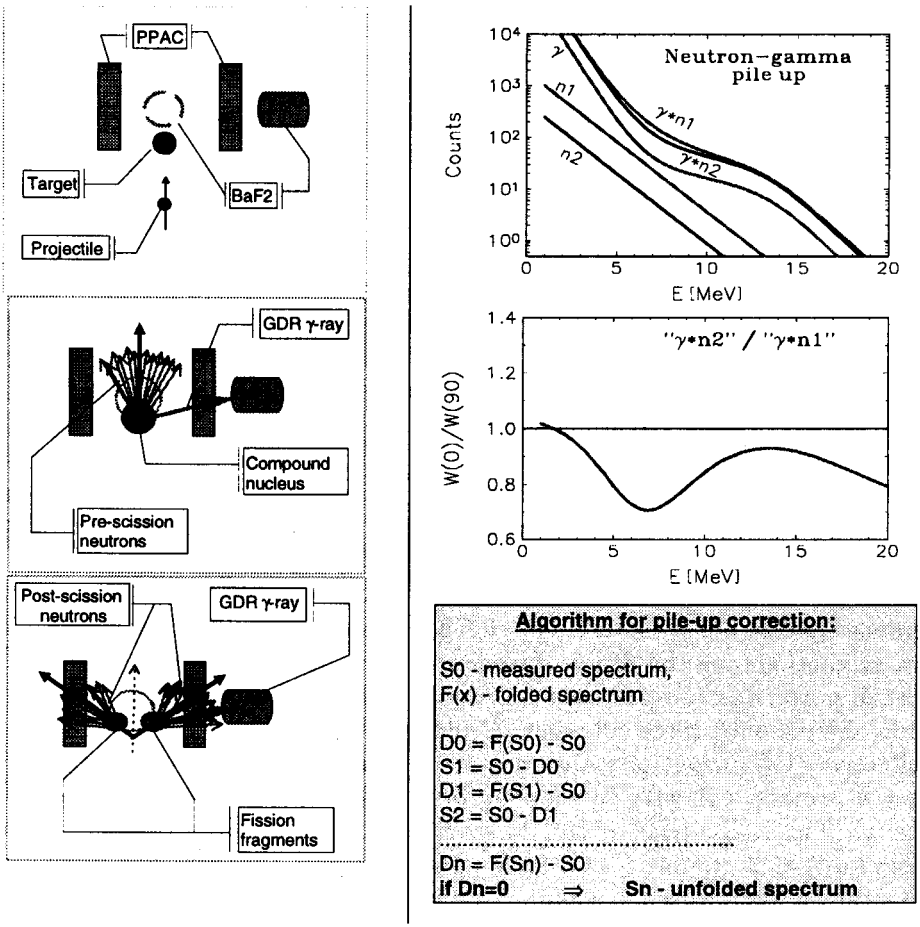

Fig. 10. Illustration of the origin of the neutron pile-up (see text for explanations).

which gamma rays and partly neutrons are measured. One BaF_2 (looking on the target through PPAC detector) reflects the experimental situation in which velocity vector of a fission fragment is parallel to the direction of the photon, and the other (looking from above): when fission fragment's velocity is perpendicular to photon's direction. The neutrons, emitted from the formed compound nucleus (the snapshot in the middle), are focused along the velocity vector of the compound nucleus and affect both BaF_2 detectors in the same amount. When fission occurs (bottom), the neutrons emitted from the fission fragments are focused along their velocity vectors and the BaF_2 detector behind PPAC detecting a fission fragment is affected much more (neutron spectrum denoted by $n1$ in the top right panel) than the

other BaF_2, looking from above (spectrum denoted by $n2$). These neutrons can pile-up with certain probability with the measured gamma spectrum (denoted by γ) and the result is shown as $\gamma * n1$ and $\gamma * n2$. The gamma spectrum in the BaF_2 detector behind the triggered PPAC (*i.e.* the spectrum of gamma rays emitted perpendicularly to the direction of the total angular momentum) is more distorted than the spectrum in the case when fission fragments hit the other pair of PPACs (gamma rays emitted parallel to the direction of the angular momentum). The resulting from this pile-up anisotropy is shown in the middle right panel. These pile-up effect can be removed using a simple algorithm [13] listed in the bottom right panel of Figure 10, providing that the neutron spectra and the probability of the pile-up are known.

The corrected anisotropy patterns for the three reactions: 15.0 MeV/u, 10.5 MeV/u (from Grenoble experiments) and 7.3 MeV/u (from Stony Brook) is presented in the upper part of Figure 11. One can see the increase of the magnitude obtained from the total spectra with increasing bombarding energy, most probably as a result of the increasing contribution of the pre-fission component.

In the bottom part of Figure 11 the anisotropy obtained from the difference spectra between 15.0 and 10.5 MeV/u is shown. The overlaid curves are predictions for the dipole emission from a nucleus with $A = 272$. The overall pattern is compatible with dipole emission from the expected liquid drop shapes with large rotation. Prolate non-collective (PNC) and oblate collective (OC) types of rotation can be excluded. The results indicate either a prolate, collectively rotating or an oblate, non-collectively rotating shape. The magnitude of the anisotropy is close to the expected asymptotic limit of 2 around $E \approx 8$ MeV. This indicates that the role of thermal orientation fluctuations is small. This might in fact be expected as the difference spectrum most likely corresponds to very high angular momenta of the compound nucleus (in this case around 100 $\hbar$ or more) which will stabilize the orientation of the nucleus [11, 14].

4.4. Lifetime estimate

Since the measured fission — γ-ray correlation has assured us that we are indeed dealing with a GDR decay, we can try, based on the results already shown in Figure 8, to estimate a lower limit for the lifetime of the hot superheavy nuclei. This can be done with a help of the excitation energy dependence of the expected lifetime for evaporation of a neutron from the compound system [2] shown in Figure 12. As we concluded from the difference spectra shown in bottom right part of Figure 8, there is no fission down to excitation energy of 210 MeV (corresponding to beam energy of 10.5 MeV/u), since there is no post-fission component present in the difference

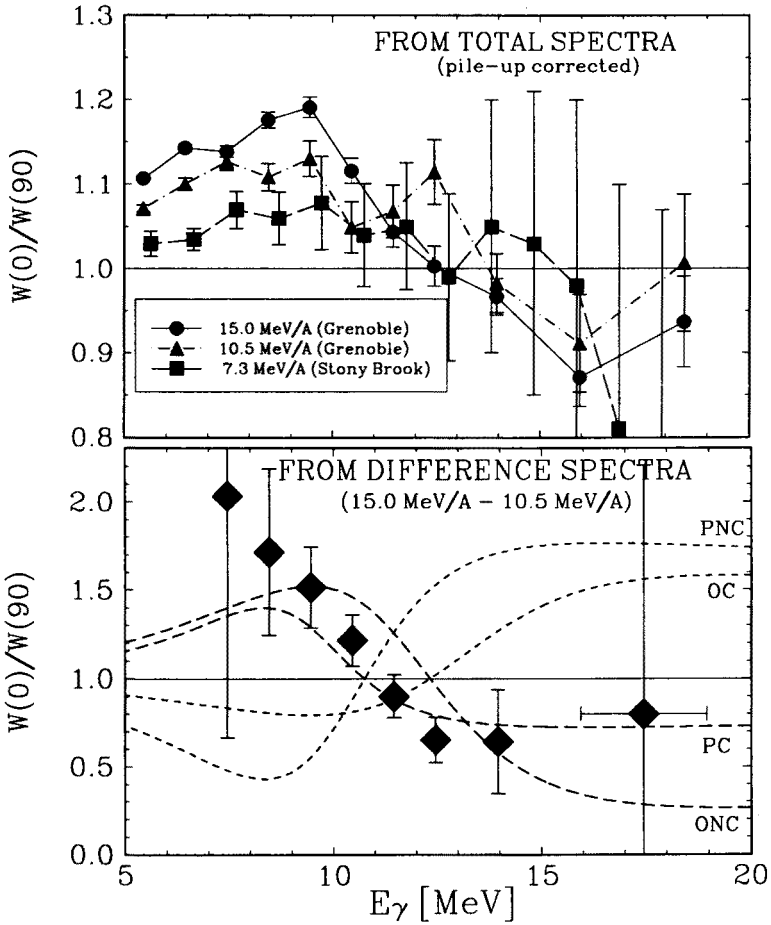

Fig. 11. The upper panel shows the comparison of the anisotropy patterns for three different bombarding energies (the lines are only to guide the eye). The bottom panel shows the anisotropy of the difference spectrum between 15 and 10.5 MeV/u. The overlaid curves are the calculation shown in Figure 9, shifted 1 MeV down the energy axis to account for the detector's response.

spectrum. The time needed for compound nucleus to cool from 380 MeV down to 210 MeV can be estimated by multiplying the average lifetime for the neutron evaporation in this energy interval (*ca.* $4 * 10^{-22}$ sec) by the average number of evaporated neutrons (that can be estimated to be about 13, as at these temperatures the neutron binding energy is about 5.5 MeV, and the average kinetic energy of the evaporated neutron is about 6 MeV). Thus the lifetime of the compound system must be at least $\tau = 5{*}10^{-21}$ sec).

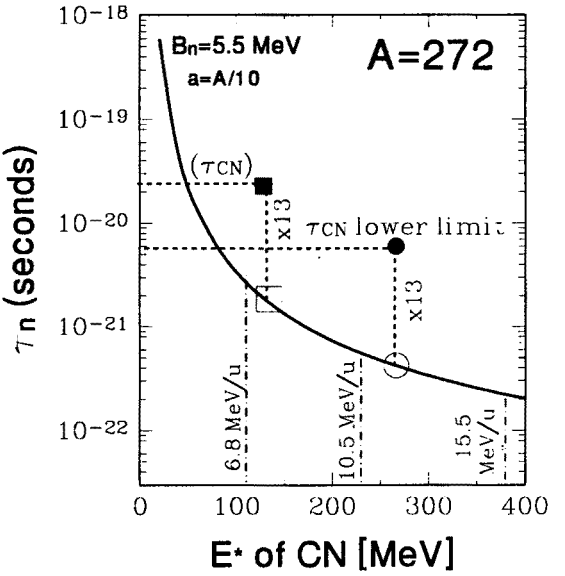

Fig. 12. Lifetime for neutron evaporation from the hot ^{272}Hs as a function of the excitation energy of the evaporating system. Deduced most probably lifetime of the compound nucleus τ_{CN} and its lower limit are indicated.

We observe still some pre-fission yield down to at least $E^* = 110$ MeV (bottom left of Figure 8). As the average number of neutrons evaporated between 210 MeV and 110 MeV is also 13 and $\tau_n \approx 2 * 10^{-21}$ sec, it means that the lifetime of the compound system must be around $\tau \approx 2.5 * 10^{-20}$ sec.

4.5. Quasi-fission

A competing process with fusion-fission is quasi-fission (fast-fission). In this scenario, the projectile, in order to overcome the saddle, has to have an additional energy, called extra-push energy. This energy is usually not high enough to make a complete fusion: the projectile is trapped behind the saddle and a so-called mononucleus is formed that lives about $5 * 10^{-21}$ sec [9, 15] and then fissions. Only if the energy of projectile is higher, requiring the so-called extra-extra-push energy, the complete fusion takes place. We tried to estimate, based on parameters from [10], what amount of quasi-fission we have in our reactions. This is illustrated in Figure 13, where we plotted the extra-extra-push energy (needed to form the compound system) and the extra-push energy (needed to form the mononucleus) as a function of angular momentum in the input channel. Also plotted are the excitation energies above the spin dependent interaction barrier for the 3 reactions studied. The crossing point of the extra-extra-push energy curve with the

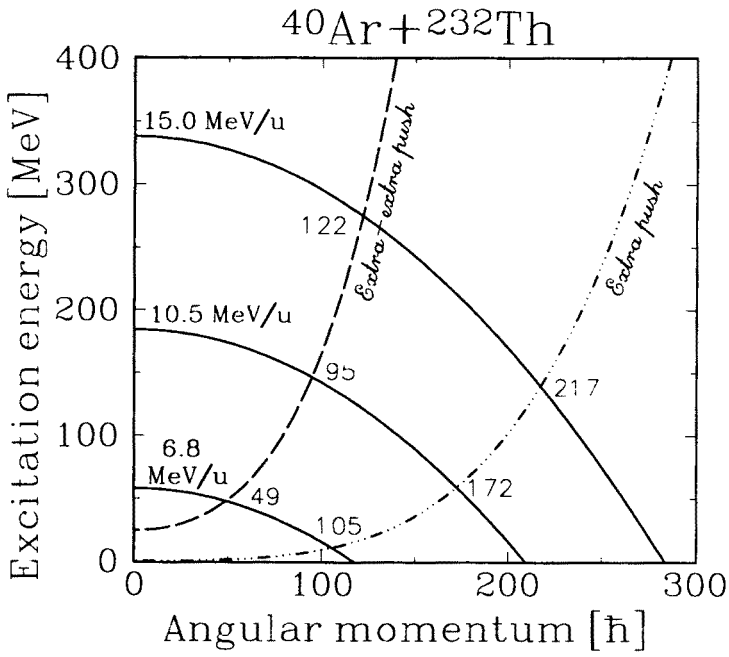

Fig. 13. Available excitation energies above the angular momentum dependent interaction barrier for the $^{40}Ar+^{232}Th$ reactions with the bombarding energies of 15.0, 10.5 and 6.8 MeV/u are shown as solid curves. Dashed and dot-dashed curves show the spin dependence of the extra-extra-push and extra-push energy, respectively.

excitation energy curve determines the highest angular momentum that can form a compound nucleus. The higher angular momenta, up to the crossing point of the extra-push curve with the excitation energy curve, are responsible for formation of the mononucleus. With these numbers we can calculate the ratio of the cross-sections for the mononucleus and compound nucleus formation. This ratio is 3.59, 2.28 and 2.16 for the 6.8, 10.5 and 15.0 MeV/u reaction, respectively. The quasi-fission is similarly to fusion-fission characterized by symmetric mass distribution but it is usually broader and it is not isotropic in the CM frame [10]. With our gating methods, described in section 4.1, we reduce the ratio of quasi-fission to fusion-fission. In fact, the difference spectrum shown in Figure 8 does not exhibit a large width, that will characterize the elongated shape of mononucleus. Nevertheless some contribution of quasi-fission in our data will not influence our conclusions. A mononucleus is assumed to be equilibrated, except shape, in all degrees of freedom, also in temperature [9]. Thus the GDR decay from the mononucleus will reflect high temperatures. Secondly, the lifetime of the mononucleus is believed to be around $5 * 10^{-21}$ sec [15]. A quasi-fission

admixture in the spectra combined with the observed lower limit for the lifetime of the system (that is a mixture of compound nuclei and mononuclei) of $\tau \approx 2 * 10^{-20}$ sec, means that the lifetime for the pure compound system must be even longer.

5. Summary and outlook

Summarizing, we can say that we can isolate the pre-fission GDR gamma decay of hot Hassium and Nielsbohrium nuclei (and their evaporation daughters) applying a difference technique. Main keys to the success of this procedure are the usage of reactions with high projectile energies, ensuring high fusion-fission cross sections, and the fact that fission is slow compared to the statistical neutron evaporation and GDR decay.

Further experiments should be able to answer in more details the questions of the deformation of the hot superheavy nucleus and of the fission dynamics (viscosity parameters). One could also speculate as to the possibility of exploiting the strongly enhanced fusion cross sections and the rather long fission lifetimes to populate the predicted island (or peninsula) of stable superdeformed nuclei around $Z = 114$ using energetic heavy ions reaction forming highly excited nuclei.

REFERENCES

[1] K.A. Snover, *Annu. Rev. Nucl. Part. Sci.* **36**, 545 (1986), and references therein.
[2] J.J. Gaardhøje, *Annu. Rev. Nucl. Part. Sci.* **42**, 483 (1992), and references therein.
[3] A. Bracco *et al.*, *Acta Phys. Pol.* **B26**, 407 (1995) and references therein.
[4] G. Viesti *et al.*, *Acta Phys. Pol.* **B26**, 393 (1995).
[5] J. Rekstadt *et al.*, *Acta Phys. Pol.* **B26**, 453 (1995).
[6] A. Bracco, J.J. Gaardhøje, A.M. Bruce, J.D. Garret, B. Herskind, M. Pignanelli, D. Barneoud, M. Maurel, H. Nifenecker, J.A. Pinston, C. Ristori, F. Schussler, J. Bacelar, H. Hofmann, *Phys. Rev. Lett.* **62**, 2080 (1989).
[7] F.S. Dietrich, J.C. Brown, W.J. O'Connel, M. Kay, *Phys. Rev.* **C10**, 795 (1974).
[8] D. Hilscher, H. Rossner, *Ann. Phys. Fr.* **17**, 471 (1992).
[9] P. Paul, M. Thoennessen, *Ann. Rev. Part. Nucl. Sci.* (1994) in press, and references therein.
[10] W.Q. Shen, J. Albiński, A. Gobbi, S. Gralla, K.D. Hildenbrand, N. Herrmann, J. Kuźmiński, W.F.J. Muller, H. Stelzer, J. Toke, B.B. Back, S. Bjørnholm, S.P. Sørensen, *Phys. Rev.* **C36**, 115 (1987).
[11] A. Maj, J.J. Gaardhøje, A. Ataç, S. Mitarai, J. Nyberg, A. Virtanen, A. Bracco, F. Camera, B. Million, M. Pignanelli, *Nucl. Phys.* **A571**, 185 (1994).

[12] J.J. Gardhøje, A. Maj, *Nucl. Phys.* **A520**, 575c (1990).
[13] T.S. Tveter, J.J. Gaardhøje, A. Ataç, J. Bacelar, A. Bracco, A. Buda, F. Camera, B. Herskind, W. Korten, W. Królas, A. Maj, A. Menthe, B. Million, H. Nifenecker, M. Pignanelli, J.A. Pinston, H.v.d. Ploeg, T. Ramsøy, F. Schussler, G. Sletten, to be published.
[14] F. Camera, A. Bracco, B. Million, J.J. Gaardhøje, A. Maj, A. Ataç, *Phys. Lett.* **B293**, 18 (1992).
[15] W.J. Świątecki, *Nucl. Phys.* **A574** , 233c (1994) and references therein.